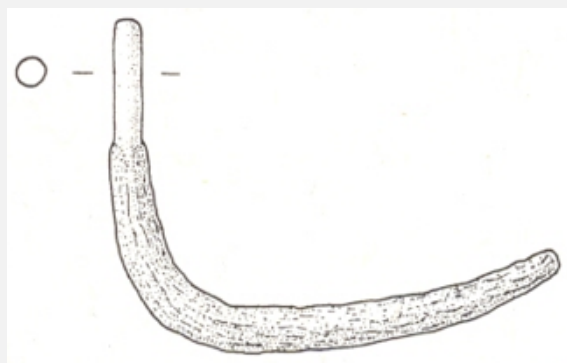


# CURVED PIN OR TANG FK 2670.20 – TIN BRONZE – LATE BRONZE AGE – SWITZERLAND

<b>Artefact name</b>	Curved pin or tang FK 2670.20
<b>Authors</b>	Marianne. Senn (EMPA, Dübendorf, Zurich, Switzerland) & Christian. Degriigny (HE-Arc CR, Neuchâtel, Neuchâtel, Switzerland)
<b>Url</b>	/artefacts/440/

## ✖ The object



Credit HE-Arc CR.

Fig. 1: Tin bronze curved pin or tang (after Fischer 1997, plate 43),

## ✖ Description and visual observation

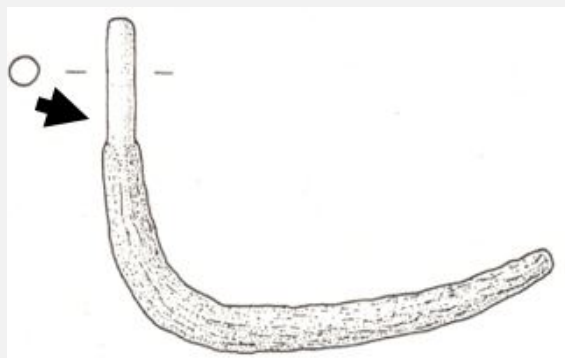
<b>Description of the artefact</b>	Curved pin or tang (Fig. 1). Several samples were taken. Only one is presented here (Fig. 2). The metal is covered with black corrosion products attributed to a burning process mixed with green corrosion products. Dimensions: L = 114mm; Ø = 4.6mm; WT = 16.7g.
<b>Type of artefact</b>	Not defined
<b>Origin</b>	Steinmöri, Neftenbach / Dorf Neftenbach, Zurich, Switzerland
<b>Recovering date</b>	Excavation in 1991?, grave 18
<b>Chronology category</b>	Late Bronze Age
<b>chronology tpq</b>	<input type="text" value="1400"/> B.C. ▼
<b>chronology taq</b>	<input type="text" value="1300"/> B.C. ▼
<b>Chronology comment</b>	14th Century BC, Bronze Age D
<b>Burial conditions / environment</b>	Soil
<b>Artefact location</b>	Kantonsarchäologie, Dübendorf, Zurich
<b>Owner</b>	Kantonsarchäologie, Dübendorf, Zurich

Inv. number FK 2670.20  
Recorded conservation data Not conserved

#### Complementary information

Nothing to report.

#### Study area(s)



Credit HE-Arc CR.

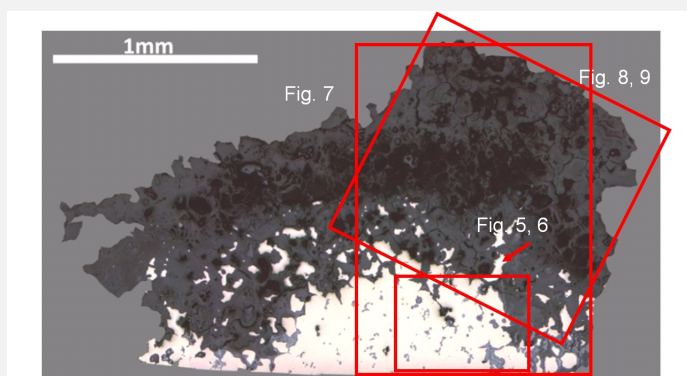
Fig. 2: Location of sampling area,

#### Binocular observation and representation of the corrosion structure

Stratigraphic representation: none.

#### MiCorr stratigraphy(ies) – Bi

#### Sample(s)



Credit HE-Arc CR.

Fig. 3: Micrograph of the cross-section showing the location of Figs. 5 to 9,

#### Description of sample

The sample (Fig. 3) is a section from the pin (or tang). The metal is covered by a thick corrosion crust (blue layer adhering to the metal, topped by a green layer mixed with black corrosion products - Museum report (1992)). Dimensions: L = 1.8mm; W = 1.2mm.

<b>Alloy</b>	Tin Bronze
<b>Technology</b>	Secondary recrystallization (produced by burning)
<b>Lab number of sample</b>	MAH 92-5-4-002
<b>Sample location</b>	Musées d'art et d'histoire, Genève, Geneva
<b>Responsible institution</b>	Musées d'art et d'histoire, Genève, Geneva
<b>Date and aim of sampling</b>	1992, examination of metallography examination

#### Complementary information

Nothing to report.

#### ∨ Analyses and results

##### *Analyses performed:*

Metallography (etched with ferric chloride reagent), Vickers hardness testing, EPMA/WDS, SEM/EDS.

#### ∨ Non invasive analysis

#### ∨ Metal

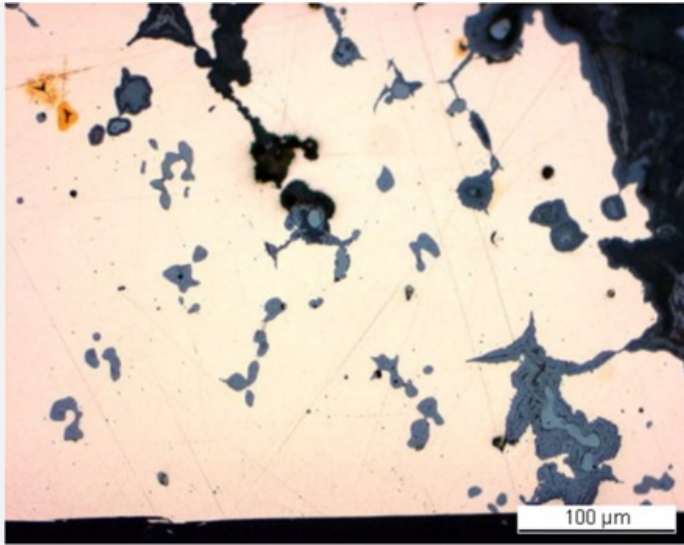
The remaining metal is a tin bronze (Table 1) with copper sulphide inclusions that contain some Fe (Figs. 5 and 6, Table 2). After etching, the tin bronze shows polygonal grains with few twins (Fig. 6). The grain size varies between 70 and 180µm indicating grain growth due to an extended or excessively hot annealing process. The copper sulphide inclusions appear in blue. The average hardness of the metal is HV1 70.

Elements	Cu	Sn	Pb	As	Sb	Fe	Zn	Ag	Au	Co	Bi	Ni	S
mass%	89.94	8.11	0.63	0.41	0.29	0.24	0.13	0.1	0.1	0.04	0.01	<	n. d.

Table 1: Chemical composition of the metal. Method of analysis: EPMA/WDS, Lab Department of Materials, University of Oxford.

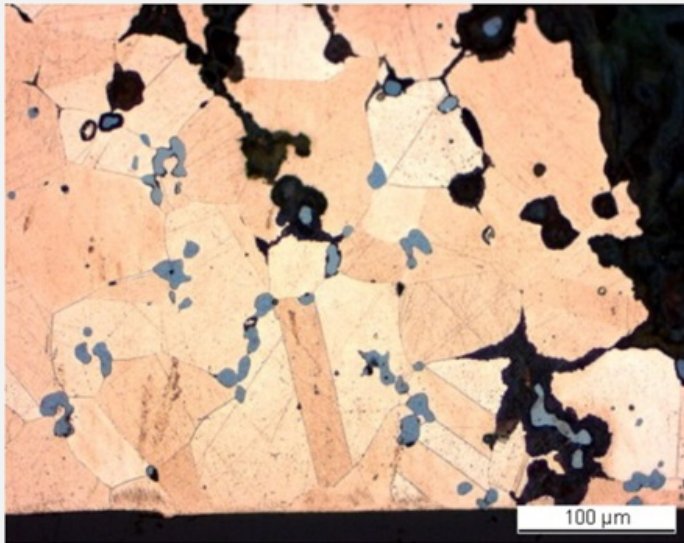
Elements	S	Fe	Cu	Total
Dark-blue inclusion	21	2.8	77	102

Table 2: Chemical composition (mass %) of the dark-blue inclusions on Fig. 4. Method of analysis: SEM/EDS, Laboratory of Analytical Chemistry, Empa.



Credit HE-Arc CR.

Fig. 5: Micrograph of the metal sample from Fig. 3 (detail), unetched, bright field. In pink the metal, in light-blue the copper sulphide inclusions and in dark- blue corrosion products,



Credit HE-Arc CR.

Fig. 6: Micrograph of the metal sample from Fig. 3 (same as Fig. 5), etched, bright field. In pink the metal with few twins, in black the resin and the corrosion products, in light-blue the copper sulphide inclusions,

<b>Microstructure</b>	Large polygonal grains with few twins
<b>First metal element</b>	Cu
<b>Other metal elements</b>	Co, Zn, As, Ag, Sn, Sb, Pb, Fe

#### Complementary information

Nothing to report.

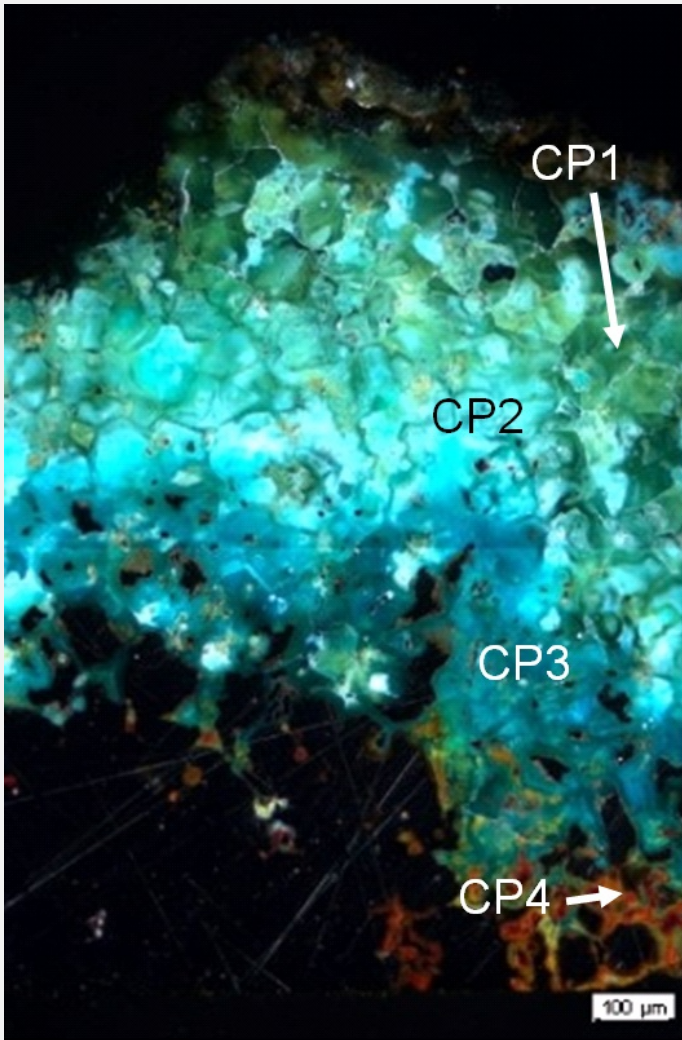
#### Corrosion layers

The corrosion crust has an average thickness of 500μm but can in areas be much thicker (Fig. 3). It is divided in two layers. The inner layer is itself divided in two sub-layers: a thin light-grey sub-layer at the interface with the remaining metal surface (CP4, in bright field) which appears red-orange in polarised light (Fig. 7) topped by a medium-grey sub-layer (in bright field) that contains remnant metal (CP3). It turns dark-blue in polarised light (Fig. 7). The outer corrosion layer can also be divided into two sub-layers: a porous sub-layer (CP2) followed by a dark-grey sub-layer in which crystals are outlined by cracks (CP1, in bright field). Under polarized light, the latter turns blue-green while on top it appears olive and brown (Fig. 7). Chemically the corrosion crust is Sn enriched and Cu-depleted (Table 3, Figs. 8 and 9). The maximum of the Sn enrichment occurs on the outer olive and brown sub-layer (CP2). The corrosion layer also contains P, Si, C and O. Inclusions containing Fe or Ag can be found in the corrosion crust (Figs. 8 and 9).

Elements	O	Cu	Sn	Si	P	Fe	Pb	S	Cl	Total
----------	---	----	----	----	---	----	----	---	----	-------

CP1, outer corrosion layer	27	17	57	1.1	1.9	0.9	1.0	<	<	105
CP3, inner corrosion layer	39	27	26	1.1	2.5	<	<	<	<	97
Remnant metal in CP3	<	88	8.3	<	<	<	<	<	<	97

Table 3: Chemical composition (mass %) of the corrosion crust from Fig. 7. Method of analysis: SEM/EDS, Laboratory of Analytical Chemistry, Empa.



Credit HE-Arc CR.

Fig. 7: Micrograph of the metal sample from Fig. 3 (detail) and corresponding to the stratigraphy of Fig. 4, unetched, polarised light. At the metal - corrosion products interface the colour of the corrosion layer is dark-blue, changing to green-blue in the outer part. The top surface of the corrosion crust is olive to brown,

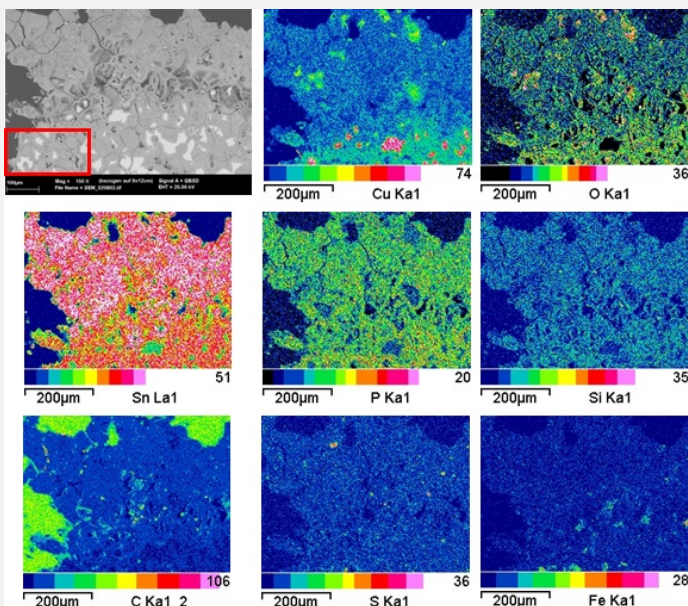
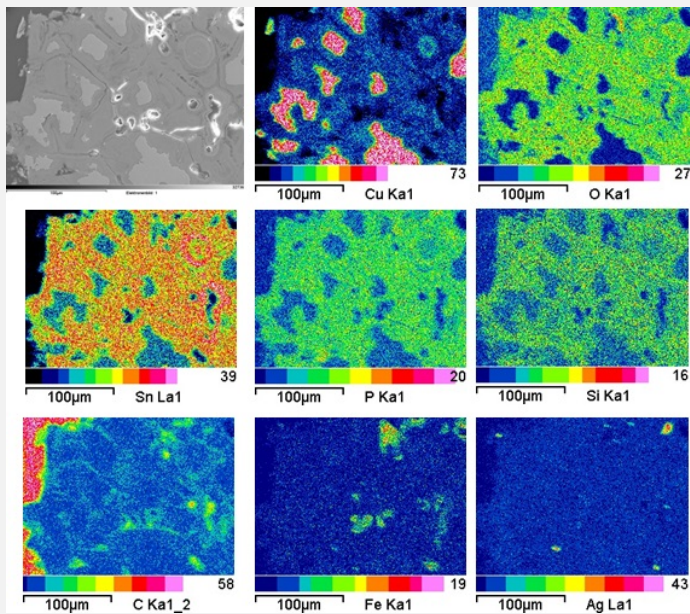


Fig. 8: SEM image, BSE-mode, and elemental chemical distribution of the selected area from Fig. 3 (due to repolishing before SEM/EDX investigation, the SEM image is slightly different from the area indicated in Fig. 3). The rectangle in the SEM image marks the detail mapping of Fig 9. Method of examination: SEM/EDS, Laboratory of Analytical Chemistry, Empa,

Credit Empa.



Credit Empa.

Fig. 9: SEM image, SE-mode, and elemental chemical distribution of the selected area from Fig. 8. Method of examination: SEM/EDS, Laboratory of Analytical Chemistry, Empa,

**Corrosion form** Uniform - intergranular

**Corrosion type** Type II (Robbiola)

#### Complementary information

Nothing to report.

#### ∨ MiCorr stratigraphy(ies) – CS

Fig. 4: Stratigraphic representation of the object in cross-section using the MiCorr application. The characteristics of the strata are only accessible by clicking on the drawing that redirects you to the search tool by stratigraphy representation. This representation can be compared to Fig. 7, Credit HE-Arc CR.

#### ∨ Synthesis of the binocular / cross-section examination of the corrosion structure

Corrected stratigraphic representation: none.

#### ∨ Conclusion

The tin bronze was exposed to an extended or excessively hot annealing process. This, combined with the extreme thickness of the corrosion crust and the dark surface, confirms that the object originates from a fire burial context. At the metal - corrosion crust interface some copper oxide (cuprite?) occurs. On top copper carbonates (azurite or malachite?) are mixed with tin oxide (cassiterite/SnO<sub>2</sub>?). Tin oxide dominates in the brown-black extremely Sn-rich outer layer. The P-enrichment in the whole corrosion layer may be due to an environment rich in organic material (for example bones). The original surface of the metal has been destroyed, presenting a type 2 corrosion layer after Robbiola et al. 1998.

*References on object and sample*

**Reference object**

1. Fischer, C. (1997) Innovation und Tradition in der Mittel- und Spätbronzezeit. Monographien der Kantonsarchäologie Zürich 28 (Zürich und Egg), 181 and plate 43.

**Reference sample**

2. Fischer, C. (1997) Innovation und Tradition in der Mittel- und Spätbronzezeit. Monographien der Kantonsarchäologie Zürich 28 (Zürich und Egg), 96.

3. Rapport d'examen 92-5-4 (Schweizer, F. and degli Agosti, M.), Laboratoire Musées d'art et d'histoire, Geneva GE (1992).

*References on analytic methods and interpretation*

4. Robbiola, L., Blengino, J-M., Fiaud, C. (1998) Morphology and mechanisms of formation of natural patinas on archaeological Cu-Sn alloys, Corrosion Science, 40, 12, 2083-2111.